Journal of Magnetic Resonance **142,** 159–167 (2000)
Article ID jmre.1999.1927, available online at http://www.idealibrary.com on IDEAL®

Electronically Tunable Surface-Coil-Type Resonator for L-Band EPR Spectroscopy

Hiroshi Hirata,[1] Tadeusz Walczak, and Harold M. Swartz[2]

Department of Diagnostic Radiology, Dartmouth Medical School, Hanover, New Hampshire 03755

Received June 3, 1999; accepted September 3, 1999

The automatic frequency control (AFC) circuit in conventional electron paramagnetic resonance (EPR) spectrometers automatically tunes the microwave source to the resonance frequency of the resonator. The circuit works satisfactorily for samples stable enough that the geometric relations in the resonance structure do not change in a significant way. When EPR signals are measured during *in vivo* experiments with small rodents, however, the distance between the signal source and the surface-coil detector can change rapidly. When a conventional AFC circuit keeps the oscillator tuned to the resonator under those conditions, the resultant frequency change may exceed ±5 MHz and markedly shift the position of the EPR signal. Such a shift results in unacceptable effects on the spectra, especially when the experimenter is dealing with narrow EPR lines. The animal movement also causes a mismatching of the resonator and the 50-ohm transmission line. Direct results of this mismatching are increased noise; shifts in the position of the baseline; and a high probability of overdriving the signal preamplifier with consequent loss of the EPR signal. We therefore designed, built, and tested a new surface-coil resonator using varactor diodes for tuning the resonance frequency to the fixed frequency oscillator and for capacitive matching of the resonator to the 50-ohm transmission line. The performance of the automatic matching system was tested *in vivo* by measuring EPR spectra of lithium phthalocyanine implanted in rats. Stability and sensitivity of the spectrometer were evaluated by measuring EPR spectra with and without the use of the automatic matching system. The overall experimental performance of the spectrometer was found to significantly improve during *in vivo* experiments using the automatic matching system. Excellent matching between the 50-ohm transmission line and the resonator was maintained under all experimental circumstances that were tested. This should allow us now to carry out experiments that previously were not possible.

Key Words: **surface coil; resonator; automatic frequency control; automatic matching control; *in vivo* EPR.**

INTRODUCTION

The automatic frequency control (AFC) widely used in continuous-wave (CW) electron paramagnetic resonance (EPR) spectrometers adjusts the frequency of microwaves to the resonance frequency of a resonator (*1*). The change of the microwave frequency, however, causes the position of the EPR spectrum to shift. If instead the resonance frequency of the resonator were tuned to a fixed microwave frequency, the EPR spectra would not be affected by the AFC. This would be particularly valuable for increasing the signal-to-noise ratio of EPR signals in animal experiments. An electronically tunable ceramic reentrant resonator for the L-band has already been developed by Chzhan *et al.* (*2*). Its resonance frequency is adjusted to a fixed microwave frequency by a voltage-controlled piezoelectric actuator. The relationship between the noise level of EPR spectra and the frequency deviation to obtain the error signal for the AFC has been discussed (*3*). To increase the sensitivity and the stability of the EPR experiments, some improved AFC systems have been reported (*4–8*).

Noise resulting from movement of animals is frequently observed during *in vivo* experiments. The movement can be due to both physiological factors (respiratory and cardiovascular) and muscular activity, especially in unanesthetized animals. This causes a mismatch between the resonator and the characteristic impedance of a transmission line (usually 50 ohm). Compensating this mismatch could significantly improve the signal-to-noise ratio in *in vivo* experiments. To keep a good match for the resonator, the coupling between the resonator and the transmission line has to be adjusted. If the CW-EPR spectrometer is equipped with an automatic matching control (AMC), the noise produced by movement can be compensated. The AMC should have a time constant that is short in comparison to the period of the movements.

There is no similar automatic matching system in "pulsed" NMR and MRI. A RF amplifier is never overdriven by the impedance mismatching between the coil and 50-ohm transmission line in a NMR spectrometer. This is because the

[1] On leave from Department of Electrical Engineering, Yamagata University, Johnan, Yonezawa, Yamagata 992-8510, Japan. E-mail: hhirata@yamagata-u.ac.jp.

[2] To whom correspondence should be addressed. E-mail: harold.swartz@dartmouth.edu.

1090-7807/00 $35.00

receiver of the spectrometer is not connected to the coil when microwave pulses are transmitted to the coil.

A variety of matching structures in NMR/MRI and EPR instruments has been reported (*9–20*). Some papers dealing with electronically controlled systems have suggested that varactor diodes be used both to tune and to match a resonator (*19, 20*). Many different surface coils have been discussed in papers dealing with NMR/MRI and EPR experiments (*21–30*). A technique for the automatic matching control of surface-coil-type resonator, however, has not yet been reported.

One problem related to use of varactors in EPR resonators is that if a varactor is in a magnetic modulation field, the applied reverse-bias voltage for the varactor will be modulated by an electromotive force. This phenomenon will result in the modulation of the matching of the resonator, and the spectrometer will be unable to distinguish this modulation from EPR signals. This unwanted modulation cannot be avoided unless the varactor and the elements supplying the reverse-bias voltages are completely shielded from the magnetic field modulation. A loop–gap type of resonator is widely used in EPR measurements, but its varactors cannot be shielded from the modulation field because the modulation field has to penetrate the resonator in order to modulate the dc magnetic field. The fundamental difference between a tunable surface-coil-type resonator presented in this article and a loop–gap resonator (LGR) is the location of the matching circuit for connecting the resonator to the spectrometer. For the tunable surface coil, the distance between the surface coil and the matching and tuning circuits is more than a half-wavelength of the electromagnetic wave employed in the measurement. For the LGR, the matching circuit (usually a coupling loop) is located in the RF electromagnetic fields. The shielding of the matching circuit for the LGR will disturb the RF magnetic field and the magnetic field modulation applied to the sample unless the matching circuit is isolated from the RF magnetic field.

This article describes an electronically tunable surface-coil-type resonator that can be used for both AFC and AMC in CW-EPR spectrometer. The principles of the resonator and the AMC are described. The theoretical background for the input impedance of the resonator is presented. The advantages of the AMC with this resonator are demonstrated in EPR measurements in a model system.

EXPERIMENTAL

Electronically Tunable Surface-Coil-Type Resonator

Figure 1 shows the configuration of an electronically tunable surface-coil-type resonator that uses varactors in its tuning and matching systems. The tunable surface coil consists of a surface coil, a parallel coaxial line formed by 50-ohm coaxial cables, and a half-wave line balun (*31*). The balun is an impedance transformer designed to couple a balanced line and an unbalanced transmission circuit (for example, a coaxial line). One varactor gives a capacitance C_{DT} for tuning the resonance frequency of the tunable surface coil. The other varactor gives the capacitance C_{DM} for changing the reactive impedance of the input impedance of the tunable surface coil. Because the capacitance of a varactor varies with the reverse-bias potential applied to it, we can adjust the resonance frequency and the reactive impedance of the tunable surface coil by adjusting the voltages applied to the varactors. Choke coils and the ceramic capacitors C_T and C_M are used for supplying the reverse-bias potential to the varactors. The choke coil connected between the center point of the balun and the ground level decreases microphonic noise produced by the magnetic modulation field. The surface coil, the parallel line, and the balun form a closed loop, and the voltage level of this loop is floated from the ground level. Since the electromotive force at the modulation frequency affects the degree of the matching between the tunable surface coil and the spectrometer, the baseline of the EPR spectrum is shifted by the modulation. The only way this modulation can be avoided is by making sure that the varactor and the elements supplying the reverse-bias potentials are completely shielded from the magnetic modulation field. We therefore contain the sensitive elements inside a solid brass casing ($\frac{1}{4}$-inch thickness).

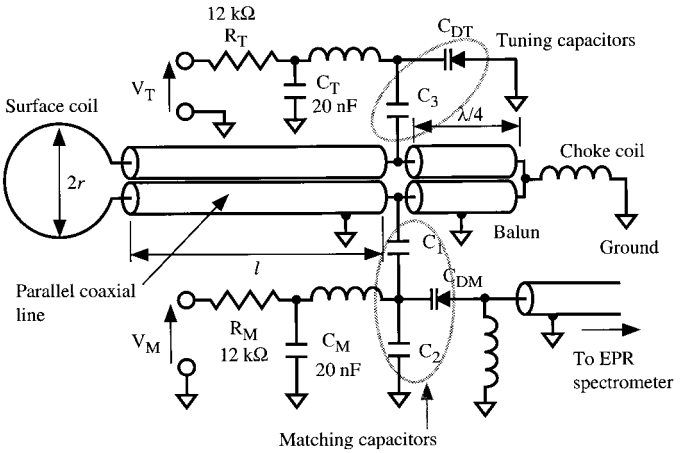

FIG. 1. Configuration of a surface-coil-type resonator with matching and tuning circuits. The length of the parallel coaxial line was 103.7 mm, the radius of the surface coil was 5.0 mm, and the thickness of wire used for the surface coil was 1.0 mm. The values of the capacitors C_1, C_2, C_3, C_T, and C_M were, respectively, 1.0 pF, 1.0 pF, 0.5 pF, 20 nF, and 20 nF. The value of the resistors R_T and R_M were 12 kΩ. The choke coils were made by quarter-wavelength thin wires, and the diameter of the choke coil was about 4.0 mm. The commercially available "semi-rigid" coaxial cables were used for the parallel line and the balun of the prototype resonator.

Automatic Frequency Control System

AFC is a conventional technique in CW-EPR spectroscopy and is therefore important for our tunable surface coil. If the

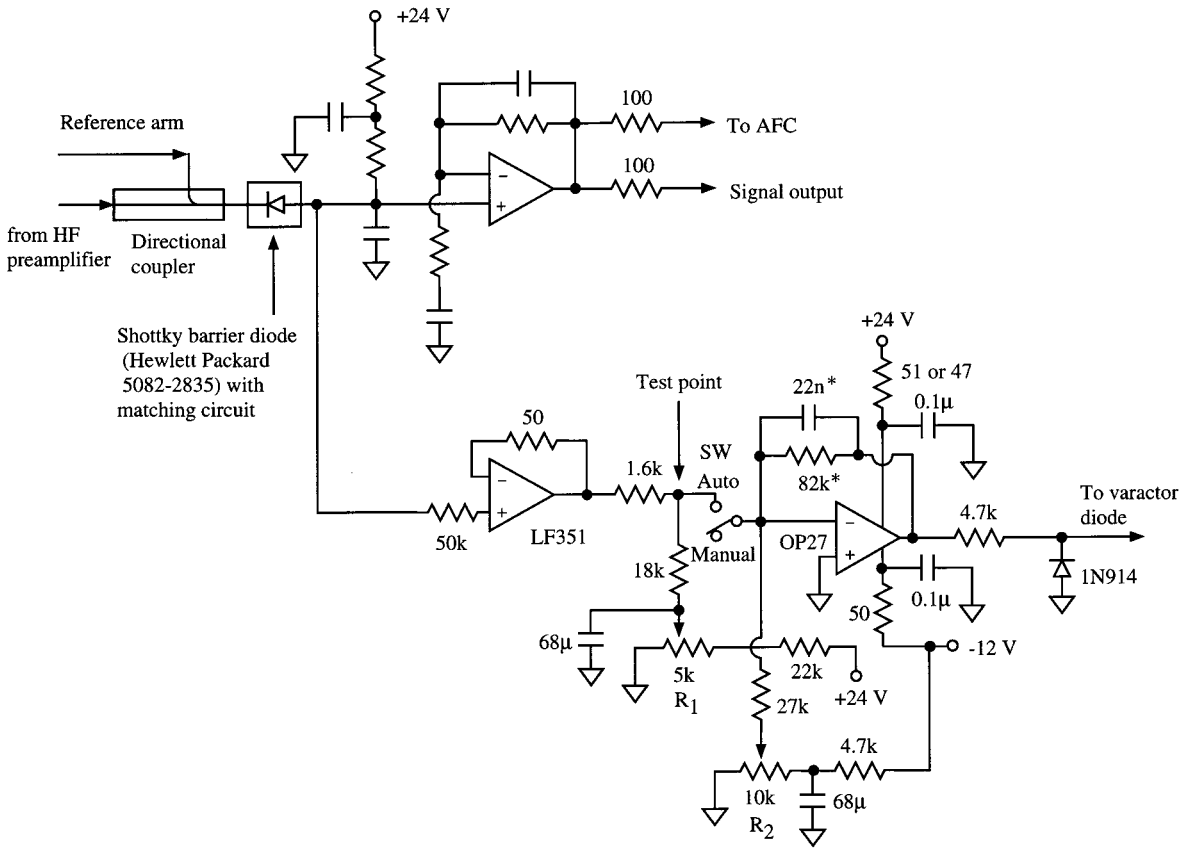

FIG. 2. An automatic matching control circuit for the tunable surface-coil-type resonator. The values of the elements marked with an asterisk are determined by the characteristics of a spectrometer.

microwave frequency is not changed by the operation of the AFC, the lineshape of the EPR signal is not affected by the action of the AFC. Almost all of the electronic circuits used in our AFC system are similar to those used in a conventional AFC system, but in our system the feedback voltage of the AFC is applied to the tunable surface coil instead of the microwave oscillator (*2*). The range over which the frequency can be controlled depends on the characteristics of the tunable surface coil. In particular, the type of varactors used and the value of capacitance connected in series with the "tuning" varactor govern the range over which the frequency can be shifted. The frequency tuning range of ± 5 MHz is necessary to obtain a good stability of the AFC for *in vivo* EPR experiments.

Automatic Matching Control System

Impedance matching between the resonator and the transmission line in EPR experiments can be adjusted by manually turning a knob to move an iris or a coupling loop or a coupling capacitor. During *in vivo* measurement, however, it is difficult to keep a good match manually and automatic matching adjustment is preferable. The degree of matching affects the amplitude and phase of the microwaves reflected from the resonator. When the transmission line has an open-circuit termination, the microwave is reflected in the same phase. When the line has a short-circuit termination, the phase of the reflected microwave is changed by 180°. The degree of matching during a measurement is obviously intermediate between the open and short terminations. If we can detect the change in the phase of the reflected wave, feedback control of the matching is possible.

Figure 2 shows our automatic matching control circuit. Phase-sensitive detection is a technique that is widely used in microwave engineering. When the phase of the reflected wave is the same as that of the reference wave, the amplitude of the summed microwaves increases. This means that the output voltage of the diode detector increases. On the other hand, when the phase of the reflected wave is opposite that of the reference wave, the output voltage of the diode detector decreases. Consequently, the phase of the reflected microwaves can be determined from this voltage shift. The voltage shift of the diode detector is amplified by the summing operational amplifier, and then the output voltage of the amplifier is fed back to the port of the matching control of the tunable surface coil. The matching is initially adjusted by using the resistive

divider to set the reference voltage in the summing operational amplifier. When the switch SW is in "manual" setting, an optimal matching can be set by a 10-turn 10-kΩ variable resistor R_2. The resistor R_1 serves to adjust the voltage at the test point to a value of 0 for ideal matching. The switch SW in the "auto" position provides an error signal for automatic matching, and the amplifier adds the output voltage of the diode detector to the reference voltage. The cutoff frequency of the AMC was 660 Hz, and it is mainly governed by the RC circuit in the input port of the tunable surface coil. This cutoff frequency is sufficient to compensate for the animal movements.

Testing of Automatic Matching Control

The performance of the AMC system was tested *in vivo* by measuring EPR spectra of lithium phthalocyanine (LiPc) implanted in rats. Two rats were tested. The effectiveness of automated matching was evaluated in the first animal while it was under general anesthesia and without any anesthesia in the second. Stability and sensitivity of the spectrometer were appraised by measuring EPR spectra with and without the AMC being active.

THEORY

Basic Design

The resonant circuit consists of the surface coil, the parallel coaxial line up to the balun, and the tuning and matching capacitor circuits. The operating frequency of the tunable surface coil was designed to have a resonance frequency appropriate to the spectrometer. Because a resonance circuit is formed by the surface coil and the parallel coaxial line, the resonance frequency of the tunable surface coil is determined by the length of the parallel coaxial line and the inductance of the surface coil. When one end of the parallel coaxial line is connected to the surface coil and the other end is an open-circuit termination, the resonance condition of the tunable surface coil is given by

$$j\omega L - jZ_{\text{parallel}}\cot \beta l = 0, \qquad [1]$$

where j is the imaginary number unit, ω is the resonance angular frequency, L is the inductance of the surface coil, and β is the phase constant of the parallel coaxial line (*32*). Two coaxial lines operate as a balanced transmission line whose characteristic impedance Z_{parallel} is given by

$$Z_{\text{parallel}} = \frac{276 \log_{10} \dfrac{b}{a}}{\sqrt{\epsilon_r}}, \qquad [2]$$

where a and b are, respectively, the inner and outer radii of the coaxial line and ϵ_r is the dielectric constant of the insulator between the inner and outer conductors.

When the resonance angular frequency is specified in advance, the line length l can be calculated as

$$l = \frac{1}{\beta} \tan^{-1}\left(\frac{Z_{\text{parallel}}}{\omega L}\right) + \frac{\lambda}{2}, \qquad [3]$$

where λ is the wavelength of electromagnetic wave in the line. Since the first term on the right-hand side of Eq. [3] is very small, the practical length of the line is obtained by adding a half-wavelength.

Formulas for Input Impedance

The half-wave line balun plays the role of a 1:2 turns-ratio transformer (*31*). The input impedance Z_{in} of the tunable surface coil is given by

$$Z_{\text{in}} = \frac{C_1 Z_1 - j\dfrac{1}{\omega}}{C_1 + C_2 + j\omega C_1 C_2 Z_1} - j\frac{1}{\omega C_{\text{DM}}}, \qquad [4]$$

where Z_1 is the load impedance at the input of the balun (the load impedance at the primary port of the transformer). The impedance at the secondary port is a combination of that due to the lumped capacitors C_3 and C_{DT} and the input impedance Z_{trans} of the parallel coaxial line. Since the voltage applied to the capacitors is half that applied to the parallel coaxial line, the load impedance Z_1 is given by

$$Z_1 = \frac{1}{4} \frac{1}{\dfrac{j\omega C_3 C_{\text{TD}}}{2(C_3 + C_{\text{TD}})} + \dfrac{1}{Z_{\text{trans}}}}, \qquad [5]$$

$$Z_{\text{trans}} = Z_c \frac{Z_L + Z_c \tanh \gamma l}{Z_c + Z_L \tanh \gamma l}, \qquad [6]$$

where γ is the propagation constant of the parallel coaxial line (*33*). Since the parallel coaxial line is a lossy line, the propagation constant should be treated as a complex number $\alpha + j\beta$. The real part α is the attenuation constant, in nepers per meter. The load impedance Z_L of the surface coil is first transformed into the input impedance Z_{trans} by the parallel coaxial line, and the impedance Z_{trans} is then transformed into the impedance Z_1 by the balun.

The load impedance of the parallel coaxial line, Z_L, is given by

$$Z_L = R_s + R_r + R_e + j\omega L, \qquad [7]$$

TABLE 1
Specifications of an Electronically Tunable Surface-Coil-Type Resonator

Radius r of surface coil	5.0 mm
Thickness t of wire used for surface coil	1.0 mm
Length l of parallel coaxial line	103.7 mm
Inner radius a of coaxial line	0.5 mm
Outer radius b of coaxial line	1.68 mm
Dielectric constant ϵ_r of the insulator between the inner and outer conductors	2.1
Attenuation constant α of coaxial line (at 1.2 GHz)	4.46×10^{-2} neper/m
Phase constant β of coaxial line (at 1.2 GHz)	36.4 rad/m
Conductivity of surface coil	5.7×10^{7} S/m
For the prototype resonator used in the measurements	
Capacitance C_1	1.0 pF
Capacitance C_2	1.0 pF
Capacitance C_3	0.5 pF

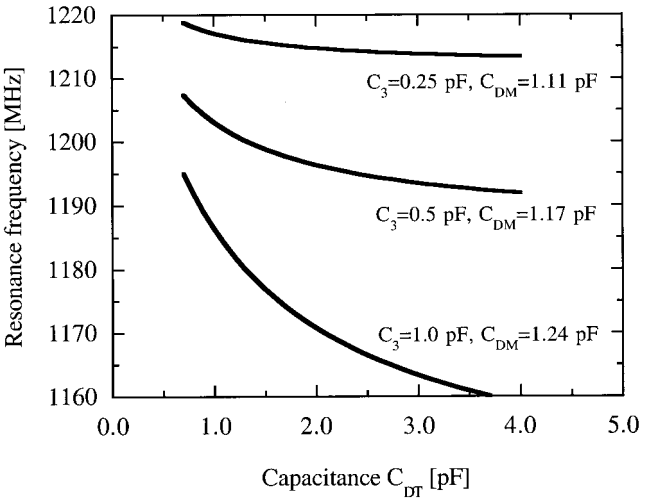

FIG. 3. Calculated resonance frequency of the surface-coil-type resonator as a function of the capacitance C_{DT}. The capacitances C_1 and C_2 were, respectively, assumed to be 0.7 and 1.0 pF.

where R_s is the ohmic resistance, R_r is the radiation resistance of the surface coil, and R_e is the equivalent resistance of the dielectric loss in the sample. These resistances can be obtained from simple assumptions (see the Appendix in Ref. [*19*]).

Numerical Calculations of Input Impedance Characteristics

The tuning and matching characteristics of a tunable surface coil whose specifications are listed in Table 1 were calculated using the formulae described in the previous section. For a surface coil 10 mm in diameter the frequency which shows the minimum reflection at the input port of the tunable surface coil is about 1.2 GHz, and the minimum reflection frequency can be calculated as a function of the tuning capacitance C_{DT}. The 1SV186 varactor diode (Toshiba, Japan) can provide a capacitance of 0.7 to 4.0 pF, and curves showing the resonance frequency over this range are shown in Fig. 3 for various values of C_3. The range of the frequency shift depends on the fixed capacitance C_3, and a frequency shift of 36 MHz should be obtained when $C_3 = 1.0$ pF. If a wide range of frequency shift is not needed, the capacitance C_3 can be small.

The matching circuit consists of two fixed capacitors and a varactor, and the degree of matching for the tunable surface coil is adjusted by changing the reverse-bias potential on the varactor. Figure 4 shows the degree of matching as a function of the capacitance C_{DM}. For a one-port junction, a scattering-matrix parameter S_{11} is defined by

$$S_{11} = 10 \log_{10} \frac{P_{ref}}{P_{in}}, \qquad [8]$$

where P_{in} is the incident power and P_{ref} is the reflected power. Thus, the scattering-matrix parameter S_{11} indicates the degree of matching. It was assumed in this calculation that the surface coil is in a vacuum. The capacitance C_{DM} which results in a good matching depends on the capacitances of the fixed capacitors. If the capacitances chosen for the matching circuit are appropriate for the samples in EPR measurement, the matching between the tunable surface coil and the transmission line is good.

RESULTS AND DISCUSSION

Tuning and Matching Characteristics

Before evaluating the performances of the AFC and AMC systems, we measured the resonance-frequency and scattering-parameter characteristics of a 1.2-GHz prototype tunable sur-

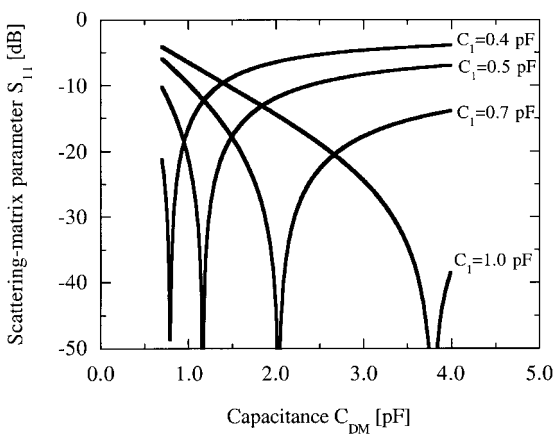

FIG. 4. Calculated results showing, for various values of C_1, the degree of matching between the surface-coil-type resonator and the transmission line as a function of the capacitance C_{DM}. The capacitances C_2, C_3, and C_{DT} were, respectively, assumed to be 1.0, 0.56, and 2.0 pF.

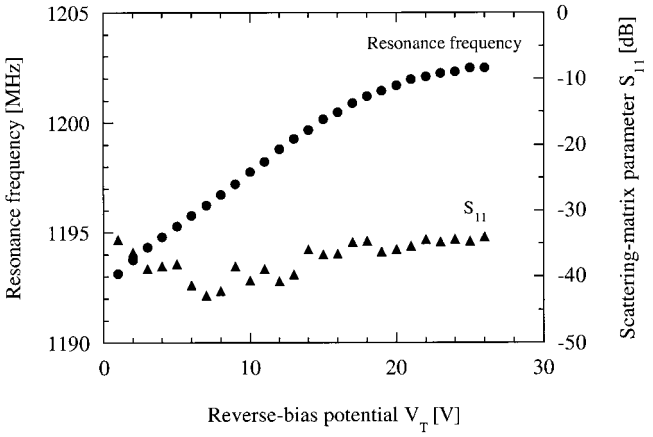

FIG. 5. Measured resonance frequency of the prototype tunable surface coil as a function of the applied reverse-bias potential V_T. The reverse-bias potential for the matching (V_M) was 18.5 V.

face coil, the specifications of which are listed in Table 1. The values of the capacitors for tuning and matching were selected to obtain a wide matching range. The scattering-matrix parameter S_{11} for the prototype tunable surface coil was measured with a vector network analyzer (Anritsu, MS620J) and a SWR bridge (Wiltron, 60NF50, directivity 46 dB).

The measured resonance frequency is shown in Fig. 5 as a function of the applied voltage V_T. When the resonance frequency was measured, the applied voltage for matching (V_M) was 18.5 V. A shift in resonance frequency of about 10 MHz was obtained. The range of the frequency shift can, as shown in Fig. 3, be adjusted by choosing a different capacitance C_3. The resonance frequency increases linearly with applied voltages up to 20 V, above which the shift in the resonance frequency shows saturation because the change of the capacitance of the varactor decreases. The low-voltage region in Fig. 5 corresponds to the large-capacitance region in Fig. 3 because the capacitance of the varactor is inversely proportional to the applied reverse-bias potential (*34*). Good matching, S_{11} more than -30 dB, was obtained throughout the wide range of the frequency shift. This decoupling between the resonance frequency and the matching is very important for the AFC system. Without it, the operation of the AFC would affect the matching during the measurement.

Figure 6 shows the matching characteristics of the prototype tunable surface coil. The resonance frequency is little influenced by differences in voltage V_M between 18 and 20 V. When the applied voltage was changed from 18 to 20 V, the frequency shift was only 320 kHz. If this frequency shift can be decreased, the AMC operation will be independent of the readjustment of the frequency. The frequency shift due to the change of matching is a fundamental limit of the present tunable surface coil. However, this shift is not a problem in practice, because the AFC simultaneously adjusts the resonance frequency of the tunable surface coil.

Compensation for Impedance Mismatching Due to Perturbation

A tunable surface coil working in a spectrometer equipped with the AFC and AMC systems was evaluated experimentally. The AFC and AMC were simultaneously working in the following experiments. Crystals of LiPc implanted in rats were used as the EPR signal source and a 1.2-GHz spectrometer was used for CW-EPR measurements. Estimates from the initial preliminary theoretical analysis are that the generated RF magnetic flux density in the surface coil is 17 μT when the applied microwave power is 25 mW. The energy dissipation in the parallel coaxial line, the balun, and the coil is, respectively, approximately $\frac{1}{2}$, $\frac{1}{4}$, and $\frac{1}{4}$ of the total energy dissipation in the tunable surface coil when the sample is not present.

Figure 7 shows typical baselines of EPR spectra collected with and without the use of AMC. This experiment was intended only to test the noise levels introduced by the automatic matching. Because the electric load of the tunable surface coil was time-invariant, even without the AMC operating the good matching of the tunable surface coil was maintained during the measurement. The root-mean-square values of the baseline are 0.090 for the top trace and 0.092 for the bottom trace in arbitrary units. These results indicate that no additional noise was added by the AMC circuit and there is no difference in the resultant baselines.

Figure 8 shows the EPR spectrum of LiPc implanted in the brain of a rat. The rat was unanesthetized in this measurement. The rat was constrained by a plastic tube and was able to sometimes move its head. The surface coil was touching the head of the rat. In the top trace measured without the AMC, the rat moved significantly when the scan reached the magnetic field of 412.8 G. The measured signal contains a spike due to the significant movement of the rat. The perturbation by this

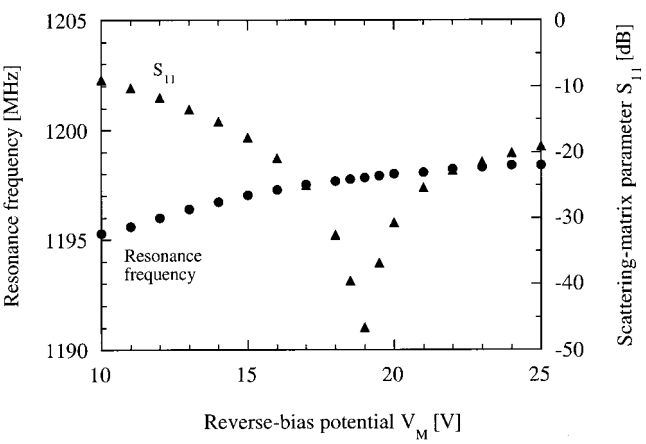

FIG. 6. Scattering-matrix parameter S_{11} (for the matching between the prototype tunable surface coil and a 50-ohm transmission line) as a function of the applied reverse-bias potential V_M when the reverse-bias potential for tuning (V_T) was 10 V.

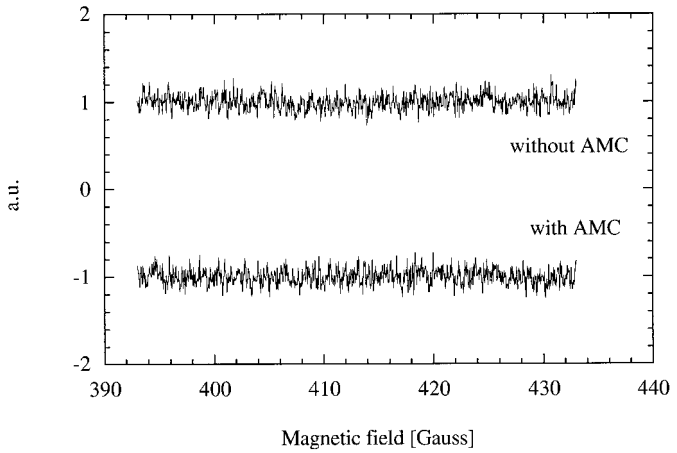

FIG. 7. Typical baselines of EPR spectra collected with and without the use of AMC. The bottle containing physiological saline solution was not moving and the EPR signal source was absent. The measurement conditions are as follows: microwave power 25 mW, sweep time 10.0 s, scan range 40.0 G, magnetic field modulation 0.2 G, and time constant 20 ms.

movement exceeded the dynamic range of a RF amplifier and, as a result, an EPR signal could not be discerned due to saturation of the RF amplifier. The bottom trace was measured with the AMC on. In this case, the measured spectrum does not show spikes such as those evident in the top trace. Even when the experimental animal moved significantly, the good impedance matching between the tunable surface coil and the transmission line was maintained by the AMC. Therefore measurement could be continued over a long period of time without readjusting the matching, even though the rat often moved in that time span.

Figure 9 shows the EPR spectrum of LiPc implanted under the skin on the neck of a rat. The rat was anesthetized in this measurement; however, the movement due to the respiration of the rat could not be avoided. The movement of the rat caused impedance mismatching between the tunable surface coil but the impedance mismatching due to the respiration was within the dynamic range of the RF amplifier and therefore the signal was not lost entirely (compare with Fig. 8). When the AMC was turned on, the noise level visible in the baseline decreased. While in fMRI it has been found that some of the "noise" actually reflected resolvable physiological processes (and therefore with proper analysis could add important information), this is unlikely to be the case for the noise attributed to physiological motions of animals in our *in vivo* measurements. The effects of the motion predictably lead to most or all of the noise that is observed. It does seem possible that when the effects of motions in the animal are sufficiently minimized by the AMC and other means, we then will be able to resolve some true physiological fluctuations of pO_2 that are currently obscured by the noise. The root-mean-square value of the noise in the top trace without the AMC is 0.325 in arbitrary units while the value for the bottom trace with the AMC is 0.230. The 300 measured points from 408 to 411 G were used for this computation. We conclude that the noise level in the baseline of the bottom trace was reduced about 30% in comparison with the top trace. The decrease of 30% for the noise level means an improvement of about 40% for the signal-to-noise ratio in this measurement ($S/(1.0 - 0.3)N \approx 1.4\ S/N$, where S is the signal amplitude, and N is the noise amplitude). Although the absolute sensitivity of the spectrometer did not improve, the practical sensitivity in *in vivo* measurements did. This is because the AMC was able to maintain good impedance matching during the measurement. Both measurements were made within an interval of a few minutes. There was no difference in the animal physiology for both measurements. Since the reflected microwaves were reduced by maintaining a good impedance matching, the noise level of the baseline was improved.

Although these studies were done with a specific type of resonator, the AMC is expected to be a useful technique for all *in vivo* EPR measurements. The resonator used in this study has no exceptional sensitivity to physiological movements of animals; we are not aware of other types of resonators that are

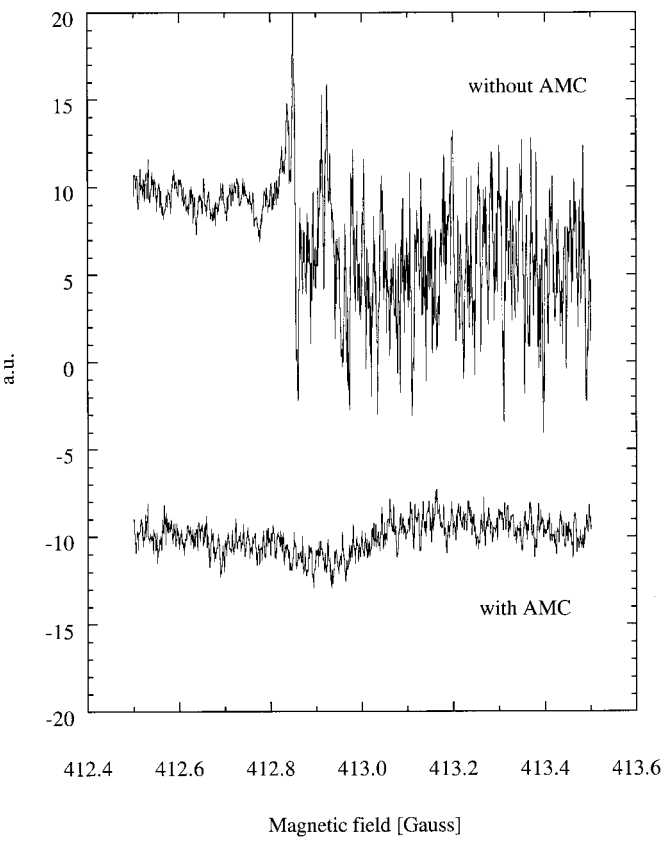

FIG. 8. EPR spectra of an unanesthetized rat with lithium phthalocyanine (LiPc) implanted in the brain. The rat was constrained by a plastic tube. The measurement conditions were as follows: microwave power 25 mW, sweep time 5.0 s, scan range 1.0 G, magnetic field modulation 0.1 G, and time constant 20 ms.

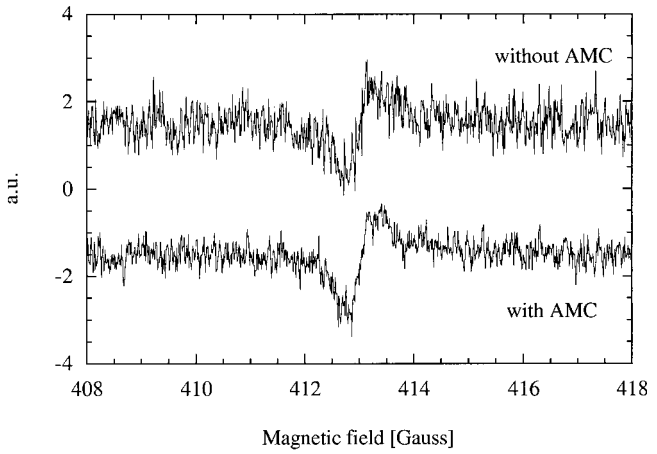

FIG. 9. EPR spectra of an anesthetized rat with lithium phthalocyanine (LiPc) implanted under the skin of the neck. The experimental conditions are as follows: microwave power 25 mW, sweep time 10.0 s, scan range 10.0 G, magnetic field modulation 0.25 G, and time constant 10 ms.

significantly less susceptible to effects of motion of animals. An important potential advantage of the automatic matching system is that it can facilitate EPR studies of unanesthetized animals. Typically, experimental animals are anesthetized before EPR measurements in order to reduce motion, but the anesthetics are likely to affect the biological phenomena being tested. The AMC therefore could significantly extend the types of useful experiments that could be done with *in vivo* EPR.

ACKNOWLEDGMENTS

The authors thank Dr. Oleg Grinberg and Dr. Artur Sucheta for their help with the *in vivo* measurements and Dr. Fraser Robb for his valuable comments on our manuscript. This research was supported in part by the Ministry of Education, Science, Sports, and Culture in Japan, a Grant-in-Aid for Encouragement of Young Scientists (10750308), and the EPR Center for the Study of Viable Systems supported by NIH Grant RR11602.

REFERENCES

1. C. P. Poole, "Electron Spin Resonance: A Comprehensive Treatise on Experimental Techniques, Second Edition," Chap. 3, p. 87, Dover Publications, New York (1983).
2. M. Chzhan, P. Kuppusamy, and J. Zweier, Development of an electronically tunable L-band resonator for EPR spectroscopy and imaging of biological samples, *J. Magn. Reson. B* **108,** 67–72 (1995).
3. M. Alecci, S. J. McCallum, and D. J. Lurie, Design and optimization of an automatic frequency control system for a radiofrequency electron paramagnetic resonance spectrometer, *J. Magn. Reson. A* **117,** 272–277 (1995).
4. S. L. Dexheimer and M. P. Klein, Sensitivity improvement of a Varian E-109 EPR spectrometer with a low noise microwave amplifier, *Rev. Sci. Instrum.* **59,** 764–766 (1988).
5. J. S. Hyde and J. Gajdzinski, EPR automatic frequency control circuit with field effect transistor (FET) microwave amplification, *Rev. Sci. Instrum.* **59,** 1352–1356 (1988).
6. P. Lesniewski and J. S. Hyde, Phase noise reduction of a 19 GHz varactor-tuned Gunn oscillator for electron paramagnetic resonance spectroscopy, *Rev. Sci. Instrum.* **61,** 2248–2250 (1990).
7. M. J. Pechan, J. Xu, and L. D. Johnson, Automatic frequency control for solid-state sources in electron spin resonance, *Rev. Sci. Instrum.* **63,** 3666–3669 (1992).
8. R. W. Quine, G. A. Rinard, B. T. Ghim, S. S. Eaton, and G. R. Eaton, A 1-2 GHz pulsed and continuous wave electron paramagnetic resonance spectrometer, *Rev. Sci. Instrum.* **67,** 2514–2527 (1996).
9. J. R. Anderson, R. A. Venters, M. K. Bowman, A. E. True, and B. M. Hoffman, ESR and ENDOR applications of loop-gap resonators with distributed circuit coupling, *J. Magn. Reson.* **65,** 165–168 (1985).
10. M. Decorps, P. Blondet, H. Reutenauer, and J. P. Albrand, An inductively coupled, series-tuned NMR probe, *J. Magn. Reson.* **65,** 100–109 (1985).
11. W. Froncisz, A. Jesmanowicz, and J. S. Hyde, Inductive (flux linkage) coupling to local coils in magnetic resonance imaging and spectroscopy, *J. Magn. Reson.* **66,** 135–143 (1986).
12. P. L. Kuhns, M. J. Lizak, S.-H. Lee, and M. S. Conradi, Inductive coupling and tuning in NMR probes; Applications, *J. Magn. Reson.* **78,** 69–76 (1988).
13. T. Ichikawa, H. Yoshida, and J. Westerling, Coupling structure for the loop–gap resonator, *J. Magn. Reson.* **85,** 132–136 (1989).
14. K. Yoda and M. Kurokawa, Inductive coupling to the slotted-tube quadrature probe, *J. Magn. Reson.* **81,** 284–287 (1989).
15. A. Raad and L. Darrasse, Optimization of NMR receiver bandwidth by inductive coupling, *Magn. Reson. Imaging* **10,** 55–65 (1992).
16. G. A. Rinard, R. W. Quine, A. A. Eaton, and G. R. Eaton, Microwave coupling structures for spectroscopy, *J. Magn. Reson. A* **105,** 137–144 (1993).
17. S. Pfenninger, W. Froncisz, J. Forrer, J. Luglio, and J. S. Hyde, General method for adjusting the quality factor of EPR resonators, *Rev. Sci. Instrum.* **66,** 4857–4865 (1995).
18. H. Hirata, T. Walczak, and H. M. Swartz, An improved inductive coupler for suppressing a shift in the resonance frequency of electron paramagnetic resonance resonators, *Rev. Sci. Instrum.* **68,** 3187–3191 (1997).
19. H. Hirata and M. Ono, Impedance-matching system for a flexible surface-coil-type resonator, *Rev. Sci. Instrum.* **68,** 3528–3532 (1997).
20. H. J. Halpern, D. P. Spencer, J. van Polen, M. K. Browman, A. C. Nelson, E. M. Dowey, and B. A. Teicher, Imaging radio frequency electron-spin-resonance spectrometer with high resolution and sensitivity for *in vivo* measurements, *Rev. Sci. Instrum.* **60,** 1040–1050 (1989).
21. J. J. H. Ackerman, T. H. Grove, G. G. Wong, D. G. Gadian, and G. K. Radda, Mapping of metabolites in whole animals by ^{31}P NMR using surface coils, *Nature (London)* **283,** 167–170 (1980).
22. J. B. Miller and A. N. Garroway, NMR imaging of solids with a surface coil, *J. Magn. Reson.* **77,** 187–191 (1988).
23. O. C. Morse and J. R. Singer, Blood velocity measurements in intact subjects, *Science* **170,** 440–441 (1970).
24. M. Garwood, T. Schleich, and G. B. Mattson, Spatial localization of tissue metabolites by phosphorus-31 NMR rotation-frame zeugmatography, *J. Magn. Reson.* **60,** 268–279 (1984).
25. D. Canet, B. Diter, A. Belmajdoub, J. Brondeau, J. C. Boubel, and

K. Elbayed, Self-diffusion measurements using a radiofrequency field gradient, *J. Magn. Reson.* **81,** 1–12 (1989).

26. D. Boudot, D. Canet, and J. Brondeau, Spatial labeling by a radiofrequency field gradient. DANTE-Z profile, Probed by one-dimensional nutation imaging, *J. Magn. Reson.* **87,** 385–394 (1990).

27. H. Nishikawa, H. Fujii, and L. J. Berliner, Helices and surface coils for low-field *in vivo* ESR and EPR imaging applications, *J. Magn. Reson.* **62,** 79–86 (1985).

28. M. Ono, K. Ito, N. Kawamura, K. C. Hsieh, H. Hirata, N. Tsuchihashi, and H. Kamada, A surface-coil-type resonator for *in vivo* ESR measurements, *J. Magn. Reson. B* **104,** 180–182 (1994).

29. H. Hirata, H. Iwai, and M. Ono, Analysis of a flexible surface-coil-type resonator for magnetic resonance measurements, *Rev. Sci. Instrum.* **66,** 4529–4534 (1995).

30. H. Hirata and M. Ono, A flexible surface-coil-type resonator using triaxial cable, *Rev. Sci. Instrum.* **68,** 3595–3596 (1997).

31. R. C. Johnson, "Antenna Engineering Handbook, Third Edition," Chap. 43, McGraw–Hill, New York (1993).

32. M. F. Iskander, "Electromagnetic Fields and Waves," Chap. 7, Prentice–Hall, New Jersey (1992).

33. R. E. Collin, "Foundations for Microwave Engineering, Second Edition," Chap. 3, McGraw–Hill, New York (1992).

34. J. J. Carr, "Microwave & Wireless Communications Technology," Chap. 15, Butterworth–Heinmann, Boston (1997).